Stanford Exploration Project, Report 125, January 16, 2007, pages 189–201

Converted-wave common azimuth migration: Real data results

Daniel A. Rosales, Robert G. Clapp, and Biondo L. Biondi

ABSTRACT

The converted-wave common-azimuth migration operator (PS-CAM) and the single mode common-azimuth migration operator share the advantage that they need a 3-D prestack cube of data with four dimensions $(t, \text{cmp}_x, \text{cmp}_y, h_x)$, instead of the entire five dimensions $(t, \text{cmp}_x, \text{cmp}_y, h_x, h_y)$. The five dimensions can be reduced to four dimensions through different processes. This paper compares two images of the PS data set from the OBS acquisition on the Alba oil field in the North sea. The two images correspond to the following processes: 1. The common-azimuth migration of the data regularized using Normal Moveout. 2. The common-azimuth migration of the data regularized using PS Azimuth Moveout. The final results show that the image from the data regularized using PS Azimuth Moveout is significantly better than the images obtained the image from the data regularized using Normal Moveout.

INTRODUCTION

Multicomponent seismic data may hold a wealth of information for oil exploration and reservoir characterization. Multicomponent seismic contains energy from converted waves that is not seen in conventional seismic; therefore, the development of new techniques to process converted-wave data is important. Much progress has been made in many areas of converted-wave seismic processing, such as stacking, DMO, migration and velocity analysis (Tessmer and Behle, 1988; Iverson et al., 1989; Huub Den Rooijen, 1991; Alfaraj, 1992; Harrison, 1990). However, more advanced techniques for single-mode PP seismic still have few converted-wave counterparts.

Common-azimuth migration is an efficient and robust technique for obtaining accurate single-mode PP 3-D seismic images. This technique takes advantage of the reduced dimensionality of the computational domain. It assumes that the data have only the zero cross-line offset; that is, all the traces in the data share the same azimuth (Biondi and Palacharla, 1996). Due to the growing number of 3-D multicomponent seismic data sets in areas where an accurate processing is required to obtain better subsurface images and/or estimate rock properties, wavefield-based continuation methods, such as common-azimuth migration, for converted-wave data are of great importance and are very much needed in the oil industry today.

Rosales and Biondi (2005) introduced the PS-CAM operator. Rosales and Biondi (2002a)

first introduced the PS-AMO operator and later Rosales and Biondi (2002b) discussed the geometry regularization problem for converted-wave data. This problem is solved in the least-squares sense. Later on, Rosales and Clapp (2006) present a more accurate transformation from a 5 dimensions prestack data cube into a 4 dimensions data cube through the reduction of the crossline offset for converted-wave data.

This paper focuses on the final image and compares the results on real 3-D Ocean Bottom Seismic data PS image from the Alba oil field. The two process that we present are: 1. Normal Moveout plus stacking along the crossline direction and PS-CAM, we refer to this process as PS-NoMoRe. 2. Data reduction along the crossline direction with the PS-AMO operator and PS-CAM, we refer to this process as PS-AMORe. The final results show that the PS-AMORe method produces images with more coherent reflectors along the reservoir level. Also, geological features (i.e. channels, faults) are now clear and easy to follow and interpret after PS-AMORe.

THEORY

We review the two main processes that we use to obtain PS 3-D images. The first process is PS geometry regularization, where an irregular data cube of 5 dimensions $(t, \mathrm{cmp}_x, \mathrm{cmp}_y, h_x, h_y)$ is mapped into a regular mesh with 4 dimensions $(t, \mathrm{cmp}_x, \mathrm{cmp}_y, h_x, h_y = 0)$. The second process is PS common-azimuth migration. where we use the regular common-azimuth cube obtained using PS geometry regularization.

PS geometry regularization

Rosales and Biondi (2002a) introduce the converted-wave azimuth moveout operator. This operator transforms data from a given offset and azimuth to data with a different offset and azimuth. This operator is a sequential application of converted-wave dip moveout and its inverse. PS-AMO reduces to the known expression of AMO for the extreme case when the P velocity is the same as the S velocity. Moreover, PS-AMO preserves the resolution of dipping events and internally applies a correction for the lateral shift between the common midpoint and the common reflection/conversion point. An implementation of PS-AMO in the log-stretch frequency-wavenumber domain is computationally efficient.

For migration efficiency, we want to use a four-dimensional data cube instead of a full five-dimensional data cube. The crossline offset axis is reduced to only one element ($h_y = 0$). The traditional process uses Normal Moveout and stacking along the crossline direction to transform the data from an irregular grid to a regular grid with four axes; however, this technique does not consider the dip and the variations along the inline and crossline directions. In this paper, we use the PS-AMO operator to map the data into a regular 4-D mesh. We follow the method described first in Clapp (2006) and extended for PS data by Rosales and Clapp (2006).

We use the nearest-neighbor interpolation operator ($\mathbf{L}'$) to map the data from an irregular

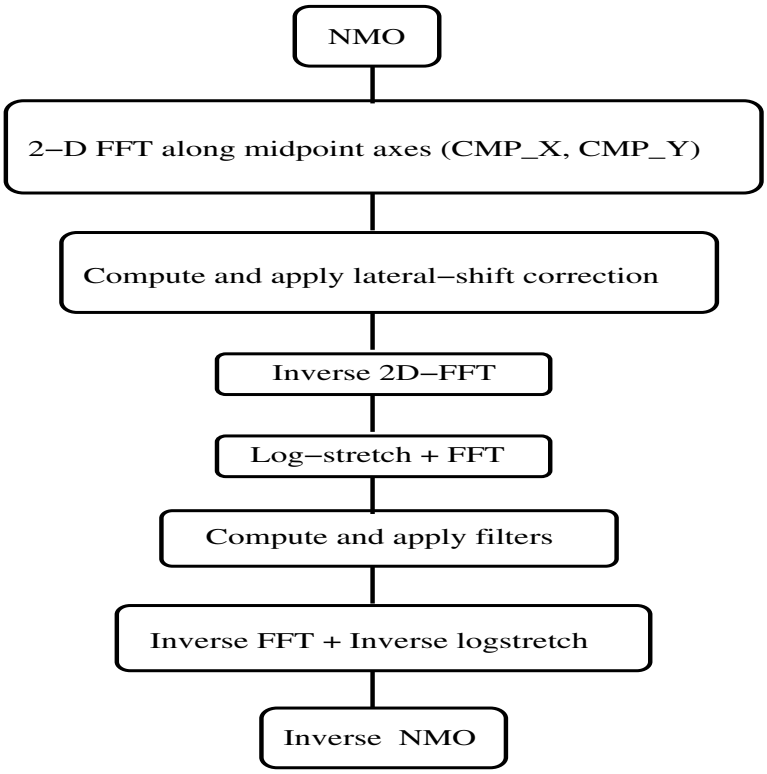

Figure 1: Diagram flow for the implementation of the PS-AMO operator. daniel1-flow [NR]

mesh into a regular mesh. The PS-AMO operator (diagramed in Figure 1) allows the transformation between various vector offsets. We use PS-AMO to transform data from $h_y \neq 0$ to $h_y = 0$. We can think of it in terms of an operator $\mathbf{Z}'$ which is a sumation over h_y. We allow for some mixing between h_x by expanding our sumation to form $h_x = a\ h_y = 0$, by summing over all h_y and

$$\sum_{a-\Delta h_x}^{a+\Delta h_x}, \tag{1}$$

where Δh_x is small.

We can combine these two operators to estimate a 4-D model ($\mathbf{m}$) from a 5-D irregular dataset ($\mathbf{d}$) through,

$$\mathbf{m} = \mathbf{Z}'\mathbf{L}'\mathbf{d}. \tag{2}$$

Equation 2 amounts to just running the adjoint of the inversion implied by,

$$Q(\mathbf{m}) = ||\mathbf{d} - \mathbf{L}\mathbf{Z}\mathbf{m}||^{\mathbf{2}}. \tag{3}$$

The adjoint solution is not ideal. The irregularity of our data can lead to artifical amplitude artifacts. A solution to this problem is to approximate the Hessian implied by equation 3 with

a diagonal matrix based on a reference model (Rickett, 2001),

$$\mathbf{m} = \mathbf{H^{-1}Z'L'd}, \tag{4}$$

where

$$\mathbf{H^{-1}} = \mathrm{diag}\left[\frac{\mathbf{Z'L'LZm}_{\mathrm{ref}}}{\mathbf{m}_{\mathrm{ref}}}\right]. \tag{5}$$

PS common-azimuth migration

The previous section describes the method we use to obtain a common-azimuth cube of PS data in a regular 4-D grid with dimensions $(t, \mathrm{cmp}_x, \mathrm{cmp}_y, h_x)$. This common-azimuth cube is the input for the PS common-azimuth operator (PS-CAM). We present a review of the PS-CAM operator introduced by Rosales and Biondi (2005).

Point-scatterer geometry is a good starting point to discuss converted-wave prestack common-azimuth migration. The equation for the travel time is the sum of a downgoing travel path with P-velocity (v_p) and an upcoming travel path with S-velocity (v_s),

$$t = \frac{\sqrt{z^2 + \|\mathbf{s}-\mathbf{x}\|^2}}{v_p} + \frac{\sqrt{z^2 + \|\mathbf{g}-\mathbf{x}\|^2}}{v_s}, \tag{6}$$

where **s** and **g** represent the source and receiver vector locations and **x** is the point-scatterer subsurface position. Common-azimuth migration is a wavefield-based, downward-continuation algorithm. The algorithm is based on a recursive solution of the one-way wave equation (Claerbout, 1985). The basic continuation step used to compute the wavefield at depth $z + \Delta z$ from the wavefield at depth z can be expressed in the frequency-wavenumber domain as follows:

$$P_{z+\Delta z}(\omega, \mathbf{k_m}, \mathbf{k_h}) = P_z(\omega, \mathbf{k_m}, \mathbf{k_h}) e^{ik_z \Delta z}. \tag{7}$$

After each depth-propagation step, the propagated wavefield is equivalent to the data that would have been recorded if all sources and receivers were placed at the new depth level (Schultz and Sherwood, 1980). The wavefields are propagated with two different velocities, a P-velocity for the downgoing wavefield and an S-velocity for the upcoming wavefield. The basic downward continuation for converted waves is performed by applying the Double-Square-Root (DSR) equation:

$$k_z\left(\omega, \mathbf{k_s}, \mathbf{k_g}\right) = \mathrm{DSR}\left(\omega, \mathbf{k_s}, \mathbf{k_g}\right) = -\sqrt{\frac{\omega^2}{v_p^2(\mathbf{s}, z)} - \mathbf{k_s}^2} - \sqrt{\frac{\omega^2}{v_s^2(\mathbf{g}, z)} - \mathbf{k_g}^2}, \tag{8}$$

or in midpoint-offset coordinates,

$$\mathrm{DSR}(\omega, \mathbf{k_m}, \mathbf{k_h}) = -\sqrt{\frac{\omega^2}{v_p^2(\mathbf{s}, z)} - \frac{1}{4}(\mathbf{k_m} - \mathbf{k_h}) \cdot (\mathbf{k_m} - \mathbf{k_h})} - \sqrt{\frac{\omega^2}{v_s^2(\mathbf{g}, z)} - \frac{1}{4}(\mathbf{k_m} + \mathbf{k_h}) \cdot (\mathbf{k_m} + \mathbf{k_h})}. \tag{9}$$

The general continuation operator can then be expressed as follows (Biondi and Palacharla, 1996):

$$\begin{aligned} P_{z+\Delta z}\left(\omega,\mathbf{k_m},k_{x_h},y_h=0\right) &= \int_{-\infty}^{+\infty} dk_{y_h} P_z\left(\omega,\mathbf{k_m},k_{x_h},y_h=0\right) e^{-ik_z\Delta z} \\ &= P_z\left(\omega,\mathbf{k_m},k_{x_h},y_h=0\right)\left\{\int_{-\infty}^{+\infty} dk_{y_h} e^{-ik_z\Delta z}\right\} \\ &\approx P_z\left(\omega,\mathbf{k_m},k_{x_h},y_h=0\right) A\left(\omega,\mathbf{k_m},k_{x_h}\right) e^{-i\widehat{k_z}\Delta z}. \end{aligned} \tag{10}$$

Since common-azimuth data is independent of k_{y_h}, the integral can be pulled inside and analytically approximated by the stationary-phase method (Bleinstein, 1984). The application of the stationary-phase method is based on a high-frequency approximation. Rosales and Biondi (2005) present the stationary-path approximation for converted-wave data.

The expression for $\widehat{k_z}$ comes from substituting the stationary-path approximation into the expression for the full DSR equation (9):

$$\widehat{k_z} = \mathrm{DSR}\left[\omega,\mathbf{k_m},k_{h_x},\widehat{k}_{h_y}(z),z\right] \tag{11}$$

where

$$\widehat{k}_{h_y}(z) = k_{ym}\frac{\sqrt{\frac{\omega^2}{v_s^2(\mathbf{g},z)}-\frac{1}{4}(k_{xm}+k_{xh})^2}-\sqrt{\frac{\omega^2}{v_p^2(\mathbf{s},z)}-\frac{1}{4}(k_{xm}-k_{xh})^2}}{\sqrt{\frac{\omega^2}{v_s^2(\mathbf{g},z)}-\frac{1}{4}(k_{xm}+k_{xh})^2}+\sqrt{\frac{\omega^2}{v_p^2(\mathbf{s},z)}-\frac{1}{4}(k_{xm}-k_{xh})^2}}. \tag{12}$$

The combination of the PS geometry regularization method and PS common-azimuth migration produces the final image from a converted-wave data set.

REAL DATA RESULTS

We use a portion of the real data set from the Ocean Bottom Seismograph (OBS) acquisition above the Alba oil field. The Alba oil field is located in the UK North Sea and elongates along a NW-SE axis. The oil reservoir is 9 km long, 1.5 km wide, and up to 90 m thick subsea (Newton and Flanagan, 1993). The 3-D OBS data set has been already preprocessed and separated into a PP and a PS section. The subset of the data set consists of 250 inline CMPs, 50 crossline CMPs, 200 inline half-offset, and 40 crossline half-offset.

This section compares the result of the traditional method with the proposed method. The traditional method uses Normal moveout plus stacking to obtain the common-azimuth data cube, followed by PS common-azimuth migration, we refer to this method as PS-NoMoRe. The proposed method uses the data regularized using PS-AMO followed by PS common-azimuth migration, we refer to this method as PS-AMORe.

Figure 2 shows the first comparison between the PS-NoMoRe result (left) and the PS-AMORe result (right). From top to bottom four depth slices at 300, 400, 500, 600 m. Note

that the acquisition artifacts are stronger in the PS-NoMoRe result than in the PS-AMORe result. At a depth of 600 m the acquisition artifacts are no longer present in the PS-AMORe result.

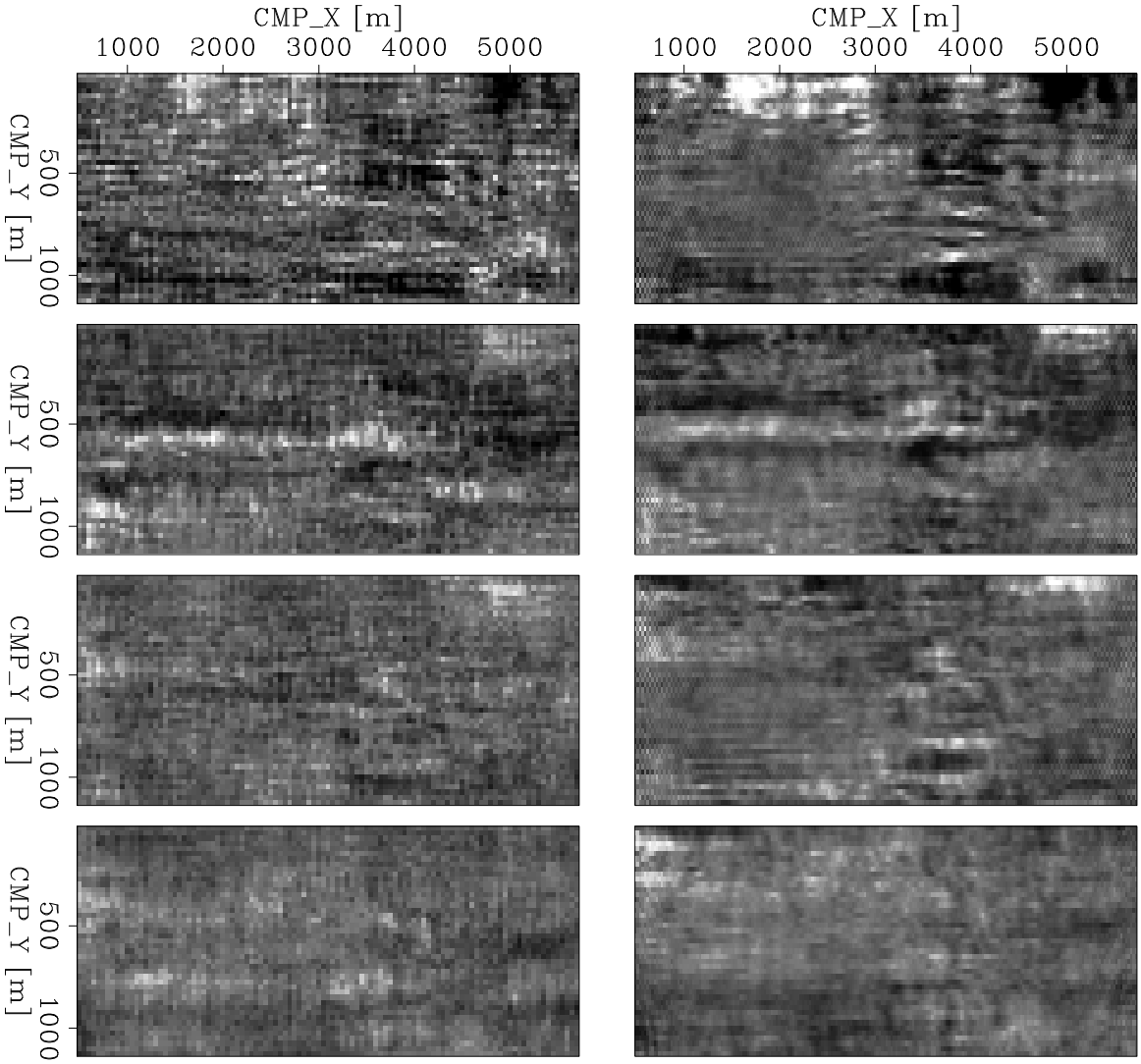

Figure 2: Comparison for several depth slices, of the PS-NoMoRe result (left) and the PS-AMORe result (right). Note how the acquisition artifacts are healed in after the PS-AMO correction and they are gone at a shallower depth with respect to the NMO correction. daniel1-ps_zslice_comp2 [CR]

The following results and comparison focus between the relative depths from 0 m and 1300 m. Figures 3 and 4 correspond to the PS-NoMoRe and the PS-AMORe results, respectively. The ovals marked as "A" in the inlines present events that are stronger in the PS-AMORe result and are not present in the PS-NoMoRe result. Note first at the very top of the ovals that the reflectors are more clearly defined after PS-AMORe. Right underneath the mark "A" inside the ovals there is an event in the PS-AMORe result that can not be followed in the PS-NoMoRe result. The same can be said about the main event at depth 720 right where the inline and

crossline sections intersect. The ovals marked as "B" also presents more continuity in the events using PS-AMORe, primarily the event at a depth of 720 m. The ovals marked as "C" in the depth slices shows a channel in the PS-AMORe result that is not clear using PS-NoMoRe.

Figures 5 and 6 show other sections on the PS-NoMoRe result and the PS-AMORe result, respectively. The geological feature marked by ovals "A" is better defined in the PS-AMORe result than in the PS-NoMoRe result. At the reservoir level, the ovals marked as "B" and "C" show the reservoir with better horizontal continuity and stronger amplitude after PS-AMORe process.

DISCUSSION AND CONCLUSIONS

The PS-AMO operator that we used had the advantage of not demanding data in the CRP domain. This operator, as a cascade operation of PS-DMO and its inverse, internally performs the CMP to CRP lateral-shift correction, since the PS-DMO operator does it as well. Therefore, *a priori* CRP binning was not necessary before applying azimuth moveout to converted-wave data. The PS-AMO operator had two main characteristics: 1) it preserved the resolution of the dipping events, and 2) it corrected for the spatial lateral shift of the common reflection point.

PS-AMO has several applications. In this work, we tested the operator for the problem of irregular geometries; more specifically the converted-wave portion of OBS seismic data. In this case, the geometry-regularization problem was handled in the least-squares sense.

The real data results show that the method proposed in this paper, that is, the PS-AMO geometry regularization followed by PS common-azimuth migration (PS-AMORe), produces results significantly better than the traditional process (PS-NoMoRe).

The PS-AMORe method enhances the main events in the final image, improves the continuity of the reflectors and recovers geological features that are lost with the traditional method (PS-NoMoRe).

ACKNOWLEDGMENTS

We thank John Toldi in Chevron and the partners of the Alba project for providing the dataset.

REFERENCES

Alfaraj, M., 1992, Transformation to zero offset for mode converted waves by Fourier transform: 62nd Annual Internat. Mtg., Society Of Exploration Geophysicists, Expanded Abstracts, 974–977.

Biondi, B. and G. Palacharla, 1996, 3-D prestack migration of common-azimuth data: Geophysics, **61**, 1822–1832.

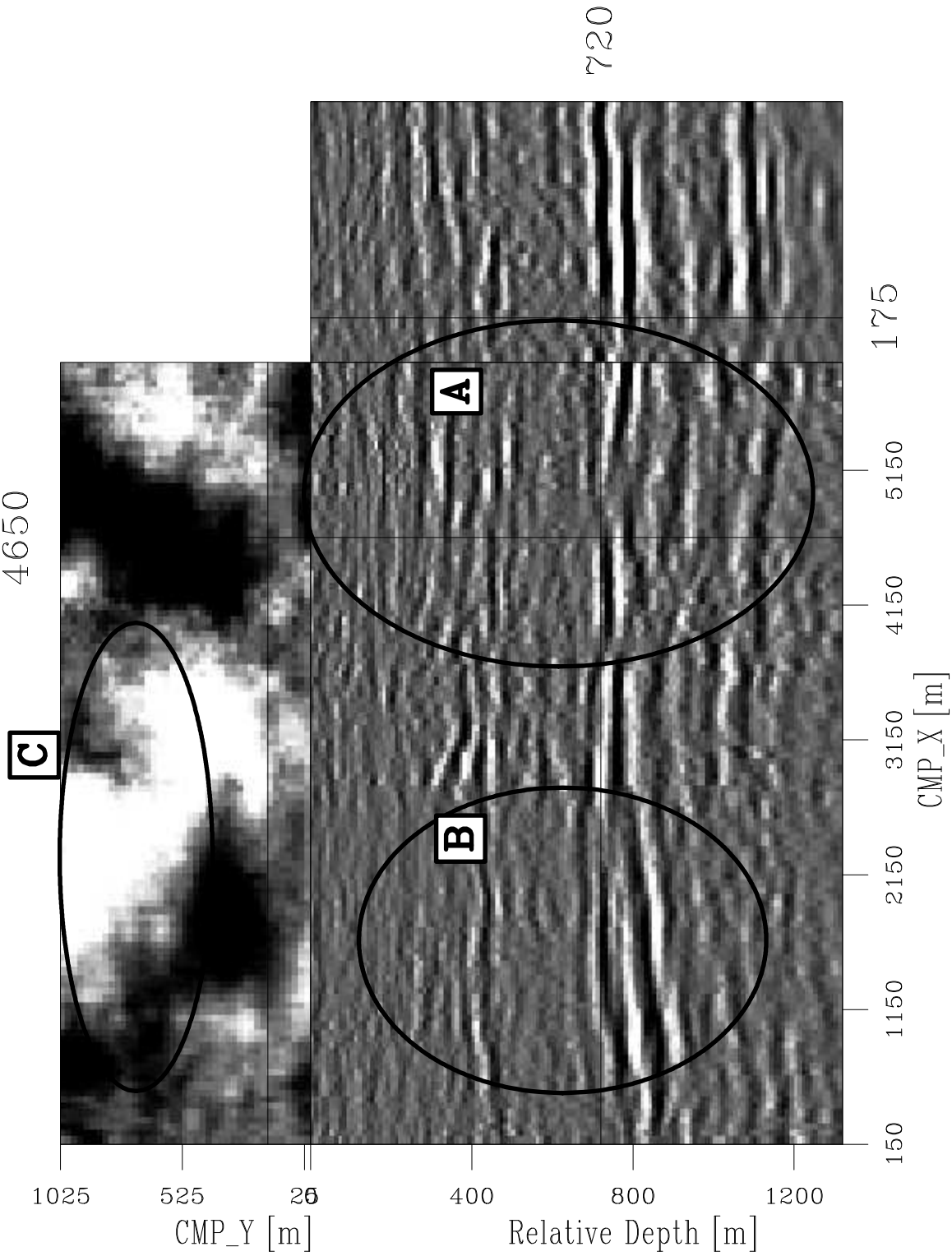

Figure 3: 3-D image displayed with depth slice at 720 m, inline section from crossline=175 m, and crossline section from inline=4650 m. This result corresponds to the PS-NoMoRe process. daniel1-ps_migstk_4_ant [CR]

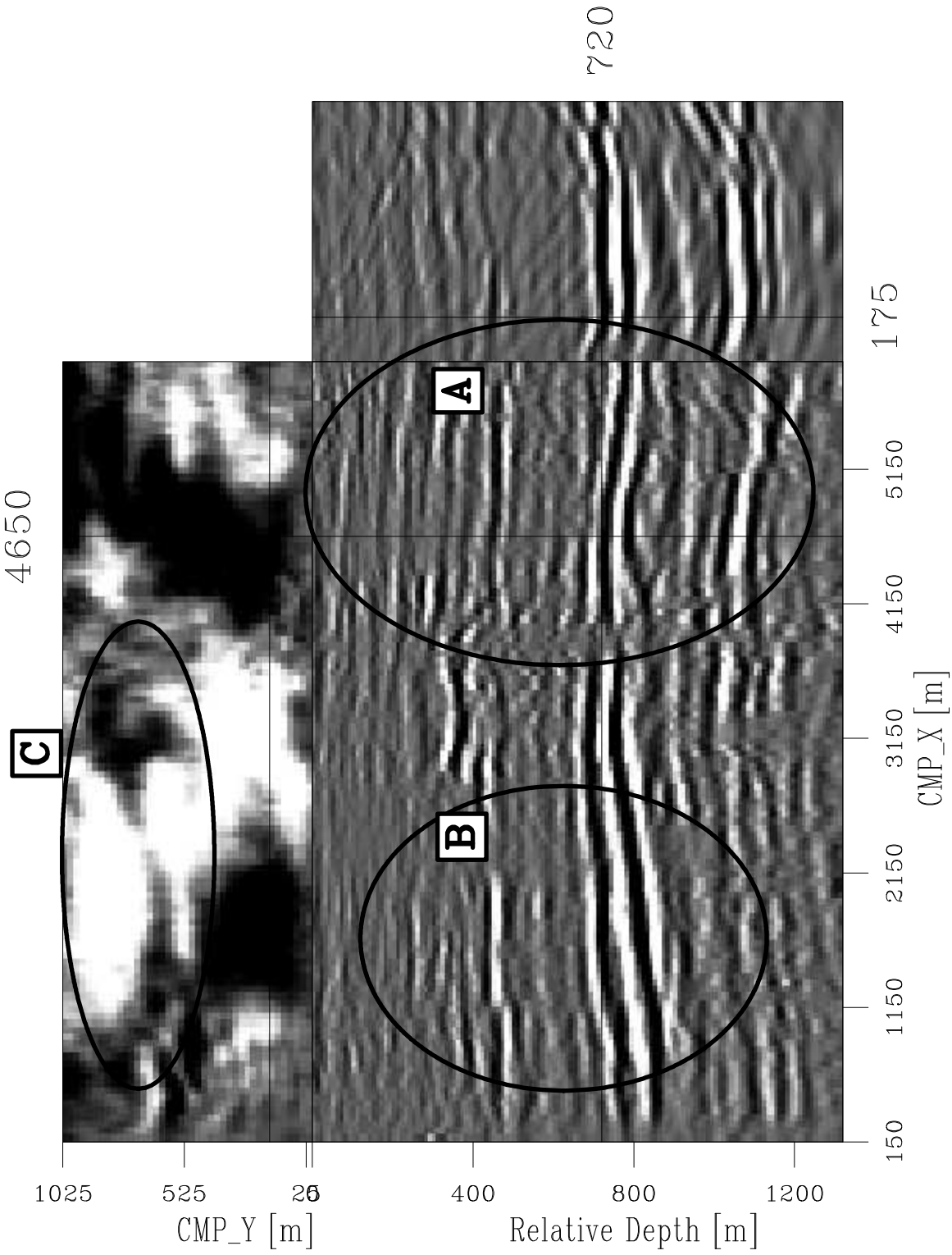

Figure 4: 3-D image displayed with depth slice at 720 m, inline section from crossline=175 m, and crossline section from inline=4650 m. This result corresponds to the PS-AMORe process. daniel1-ps_amostk2_4_ant [CR]

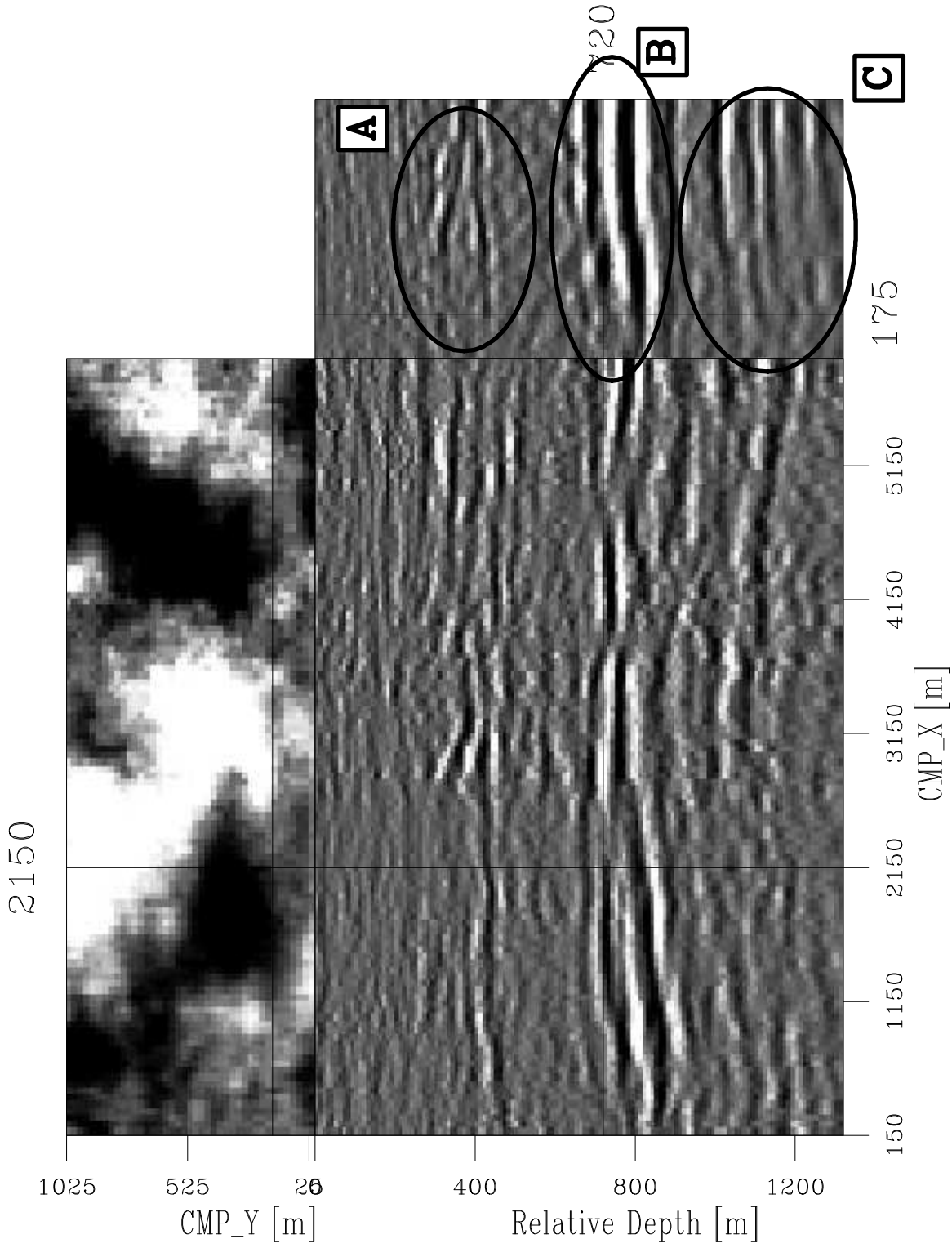

Figure 5: 3-D image displayed with depth slice at 720 m, inline section from crossline=175 m, and crossline section from inline=2150 m. This result corresponds to the PS-NoMoRe process. daniel1-ps_migstk_5_ant [CR]

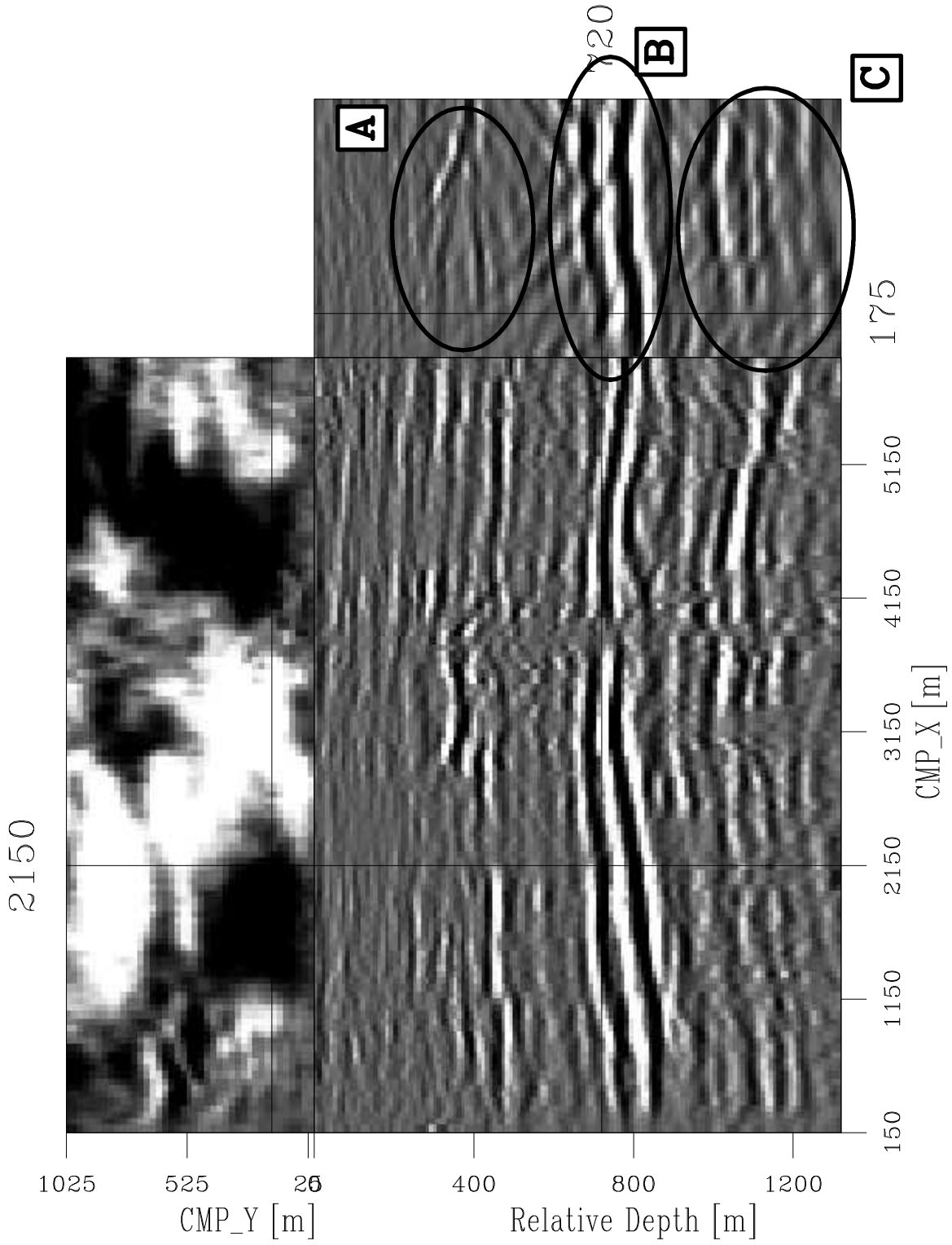

Figure 6: 3-D image displayed with depth slice at 720 m, inline section from crossline=175 m, and crossline section from inline=2150 m. This result corresponds to the PS-AMORe process. daniel1-ps_amostk2_5_ant [CR]

Bleinstein, N., 1984, Mathematical methods for wave phenomena: Academic Press.

Claerbout, J. F., 1985, Imaging the earth's interior: Blackwell Scientific Publications.

Clapp, R. G., 2006, Amo inversion to a common azimuth dataset: Field data results: SEP–**124**.

Harrison, M., 1990, Converted wave DMO: 60th Annual Internat. Mtg., Society Of Exploration Geophysicists, Expanded Abstracts, 1370–1373.

Huub Den Rooijen, P. G. M., 1991, Stacking of P-SV seismic reflection data using dip moveout: Geophysical Prospecting, **39**, no. 4, 585–598.

Iverson, W. P., B. A. Fahmy, and S. B. Smithson, 1989, VpVs from mode-converted P-SV reflections: Geophysics, **54**, no. 7, 843–852.

Newton, S. and K. Flanagan, 1993, The Alba field: evolution of the depositional model: Proceedings of the 4th conference, Geological Society, Parker , J., Petroleum Geology of Northwest Europe, 161–171.

Rickett, J., 2001, Spectral factorization of wavefields and wave operators: Ph.D. thesis, Stanford University.

Rosales, D. and B. Biondi, 2002a, Converted wave azimuth moveout: SEP–**111**, 59–71.

Rosales, D. and B. Biondi, 2002b, Multicomponent data regularization: SEP–**112**, 97–108.

Rosales, D. A. and B. Biondi, 2005, Converted-wave common-azimuth migration: SEP–**120**, 277–282.

Rosales, D. A. and R. G. Clapp, 2006, Ps - azimuth moveout: Real data application: SEP–**124**.

Schultz, P. S. and J. W. C. Sherwood, 1980, Depth migration before stack: Geophysics, **45**, 376–393.

Tessmer, G. and A. Behle, 1988, Common reflection point data-stacking technique for converted waves: Geophysical Prospecting, **36**, no. 5, 671–688.